JOURNAL OF APPLIED ELECTROCHEMISTRY 19 (1989) 377-382

Factors influencing the preferential orientations in zinc coatings electrodeposited from chloride baths

I. TOMOV, CHR. CVETKOVA, V. VELINOV

Institute of Physical Chemistry, Bulgarian Academy of Sciences, 1040 Sofia, Bulgaria

A. RIESENKAMPF*, B. PAWLIK

Institute for Metal Research, Polish Academy of Sciences, ul. Reymonta 25, 30-059 Krakow, Poland

Received 25 July 1988; revised 12 October 1988

The influence of factors affecting the texture formation in zinc coatings electrodeposited from weakly acid zinc baths has been investigated, particularly those of cathodic current density, electrolyte additives and substrate texture type. Deposits showing no preferential orientations were obtained from a chloride bath with no primary inhibitors, with which the earlier theory on autoinhibition caused by colloidal zinc hydroxide in sulphate electrolytes was confirmed. The addition of synthetic inhibitors resulted in the production of various types of texture according to the electrolysis conditions and substrate texture type. Cone fibre texture coatings were obtained on cold worked copper cathodes and at lower cathode densities. A simple fibre texture was produced only at higher D_c values. The preferential orientation of electrodeposited zinc coatings on electrolytic nickel textured substrates depended on whether the electrochemical conditions or the textured substrate was the dominant factor. Various simple fibre textures were formed on electrodeposited amorphous Ni-P alloy substrates irrespective of the electrochemical conditions. Within a relatively short time after the completion of the electrodeposition of zinc coatings from chloride or sulphate baths, recrystallization processes were observed at room temperature.

1. Introduction

There arose in our studies [1] a need for deeper investigation of the influence of electrodeposition conditions on deposit structure. It was found that zinc deposits with special structural properties are often produced in chloride or sulphate electrolytes, both with and without inhibiting additives. Along with the simple fibre textures, so-called cone textures [2] of various preferential orientations were often formed. In a number of zinc coating specimens recrystallization processes were also observed to occur at room temperature in the as-fabricated state. The clarification of the causes of this structural phenomenon is a matter of undoubted theoretical and practical interest. The present work aims to define the factors which influence the texture of coatings electrodeposited from a slightly acid chloride electrolyte under varying electrolysis conditions and on various substrates.

Table 1. Compositions of baths

Bath	Concentration ($g\,l^{-1}$)			Additives ($ml\,l^{-1}$)	
	$ZnCl_2$	NaCl	H_3BO_3	Car	Br
A	80	160	20	–	–
B	80	160	20	50	–
C	80	160	20	50	5

* Author to whom correspondence should be addressed.

2. Experimental details

The zinc coatings were obtained from baths the compositions of which are indicated in Table 1. The additives were a blend of Bulgarian technological products [1], including carrier 'Univer A', based on ethoxyalkylophenol with 10-20 ethoxy groups, and brightening agent 'Univer B', based on benzylidenacetone. Electrolytes with no additives, or with only one of them, were also examined for comparison.

The specimens for texture investigations were prepared under galvanostatic conditions at various cathodic current densities (1, 2, 4 and 8 $A\,dm^{-2}$), using a rotating disc electrode (RDE) with a rotation speed of 1.3 Hz. The cathodes were discs 30 mm in diameter prepared in different ways. The following substrates were used: (a) cold worked copper disc; (b) amorphous Ni-P film (thickness 10-15 μm), electrodeposited [3] on a brass disc; (c) crystalline nickel coating (thickness 50 μm), with fibre texture $\langle 100 \rangle$, $\langle 110 \rangle$, $\langle 210 \rangle$ or $\langle 211 \rangle$, respectively, electrodeposited [4-7] on brass discs.

This method of specimen preparation enabled us to properly recognize the substrate effect on the texture type. The pole figures were measured by means of an X-ray texture goniometer with CuK_α radiation and a nickel filter. In order to determine reliably the preferential orientation the following three pole figures were measured for each specimen: $\{10\bar{1}0\}$, $\{11\bar{2}0\}$ and $\{10\bar{1}1\}$. The amorphism of Ni-P substrates

0021-891X/89 $03.00 + .12

Table 2. Texture ⟨uv.w⟩ of zinc coatings electrodeposited on cold worked copper substrates. Thickness of the deposits ~20 μm

Specimen No.	*Bath*	*Cathodic current density D_c ($A\ dm^{-2}$)*	*Predominant orientation ⟨uv.w⟩*	*Type of texture and angle ϕ_0*	*Characteristic of texture*
1	A	2	Random	–	–
2	B	1	⟨11$\bar{2}$0⟩	Fibre text.	Sharp
3	B	4	⟨11$\bar{2}$0⟩	Fibre text.	Smeared out
4	B	8	⟨11$\bar{2}$0⟩	Fibre text.	Smeared out
6	C	1	⟨10$\bar{1}$0⟩[1] + ⟨11$\bar{2}$0⟩	Cone text. 14°	Smeared out
7	C	2	⟨10$\bar{1}$0⟩[1] + ⟨11$\bar{2}$0⟩	Cone text. 10°	
8	C	4	⟨10$\bar{1}$0⟩[1] + ⟨11$\bar{2}$0⟩	Cone text. 7°	(Fig. 1)
9	C	8	⟨10$\bar{1}$0⟩	Fibre text.	Sharp (Fig. 2)

[1]Angle ϕ_0 is referred to the given texture component.

was checked with an X-ray diffractometer by observing the so-called amorphous halo present within the range of small angles.

In order to investigate recrystallization phenomena in zinc electrodeposits, the method described in [8] was employed, using a back reflection technique.

3. Results and discussion

3.1. *Texture of zinc coatings electrodeposited on cold worked copper substrates*

Table 2 summarizes the electrodeposition conditions for zinc coatings together with the texture characteristics obtained. Without any added inhibitor, the chloride electrolyte (bath ‘A’) yielded deposits showing no preferential orientation. Thus the hypothesis [1], proposed in the study of zinc electrodeposition from sulphate solutions, was confirmed. According to this, the texture formation is influenced by zinc hydroxide generated within the cathodic layer. In the presence of chloride ions the colloidal hydroxide undergoes coagulation [9–11] and, hence, is unable to act as an inhibitor.

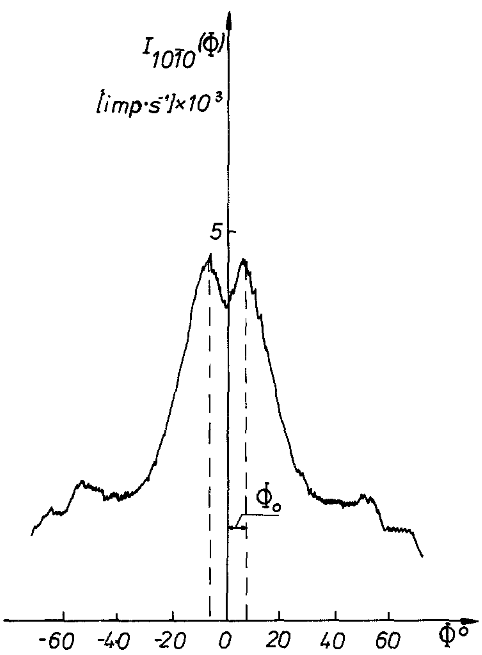

Fig. 1. Pole figure {10$\bar{1}$0} of zinc coating electrodeposited on cold worked copper substrate (sample 8, Table 2) – cone fibre texture with component ⟨10$\bar{1}$0⟩: ϕ_0 = 7°.

Layers with predominant orientations ⟨11$\bar{2}$0⟩ and ⟨10$\bar{1}$0⟩ were obtained from the electrolytes with added synthetic inhibitors (baths ‘B’ and ‘C’). Depending on the electrolysis conditions and electrolyte composition, either simple fibre textures or so called cone fibre textures (Fig. 1) were achieved. It is well known that the fibre axis direction forms an angle ϕ_0 with the ⟨uvw⟩ directions of all crystallites belonging to the given component in the latter case. These textures are known as ‘cone fibre texture’ [2], since the ⟨uvw⟩ directions of the relevant crystallites are situated in a cone with an aperture angle $2\phi_0$ about the fibre axis. The cone texture is defined by the angle ϕ_0 which is measured on the pole figure with {hkl} indices equivalent to the respective texture component.

It is evident from the results in Table 2 that the value of the ϕ_0 angle of the texture component ⟨10$\bar{1}$0⟩ measured on the pole figure {10$\bar{1}$0} decreases with the increase in current density D_c (specimens 6, 7 and 8). Therefore, it may be assumed that at sufficiently high cathode current density conditions will arise (with otherwise unchanged parameters) under which the cone texture will convert into a simple fibre texture (ϕ_0 = 0). In fact, at D_c = 8 A dm^{-2} (specimen No. 9), a simple fibre texture was obtained (Fig. 2). In order to reveal whether the growing cone texture can be converted into a simple fibre texture with a prescribed current density and bath composition, the texture was investigated as a function of the layer thickness (Table 3). To this end we prepared zinc coatings under conditions of continuous electrodeposition with thicknesses 10, 20 and 40 μm (specimen Nos. 10, 11, 12). The studies showed that the coatings had a cone texture with two components ⟨10$\bar{1}$0⟩ + ⟨11$\bar{2}$0⟩ (Fig. 3a). It was also found that the increase in the coating thickness has almost no effect on the value of the ϕ_0 angle of the ⟨10$\bar{1}$0⟩ component. A bell-shaped distribution of the poles was obtained for the {11$\bar{2}$0} pole figure. This is due to the reflections symmetrically overlapping as regards ϕ = 0 (Fig. 3b).

Other layer specimens were prepared by deposition from the same bath and at the same current density, except that the cathodic current was cut off for 5 s each 5 min in order to restore the growth layer surface. The same texture components were found in these speci-

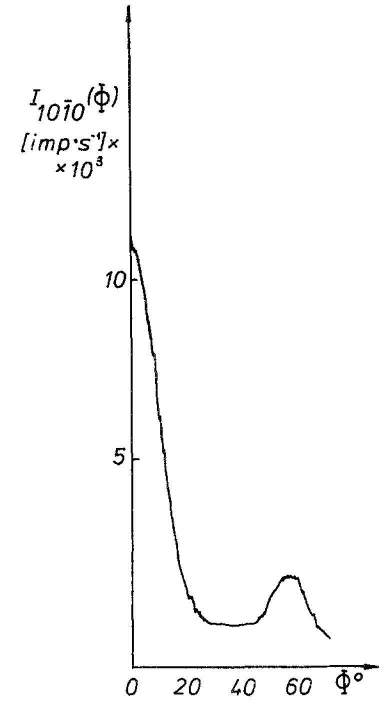

Fig. 2. Pole figure {10$\bar{1}$0} of zinc coating electrodeposited on cold worked copper substrate (sample 9, Table 2) — texture component ⟨10$\bar{1}$0⟩, sharp.

mens too (Table 3). The data presented in the table indicate the specimen texture does not convert from cone to simple fibre texture during the growth process.

These results show that the preferential orientation of crystallites in the layer is influenced both by electrolyte composition and current density. Along with these, however, an influence of the substrate texture may also be assumed. Its epitaxial effect in some cases is the most probable reason for the deposition of cone textured zinc coatings. To clarify this phenomenon studies were carried out with amorphous Ni–P alloy substrates and electrolytically deposited Ni substrates with prescribed textures.

3.2. *Texture of zinc coating electrodeposited on textured electrolytic nickel substrates*

Table 4 shows the electrodepositing conditions for zinc coatings on nickel substrates with a prescribed texture, as well as the characteristics of the achieved predominant orientations. In general, the texture type and sharpness were influenced by two factors: the substrate effect and the electrochemical conditions of the electrodeposition process. At higher cathode current densities, up to 2 or 4 A dm^{-2}, a sharp ⟨10$\bar{1}$0⟩ orientation was achieved in the zinc coating, irrespective of the substrate texture type. At a lower cathode current density, D_c = 1 A dm^{-2}, the substrate texture became a predominant factor influencing the crystallite orientations.

In the case of bath ‘C’, the competition between substrate effect and electrochemical conditions (current density) resulted in the formation of cone texture on the nickel substrates with a ⟨110⟩, ⟨100⟩ and ⟨210⟩ orientation. On the other hand, a sharp ⟨10$\bar{1}$0⟩ texture formed on a substrate of ⟨211⟩ orientation.

In the case of bath ‘B’ and substrate ⟨100⟩, a new sharp texture, containing the ⟨10$\bar{1}$1⟩ component, was produced (Fig. 4, specimen No. 37). In both cases, the reason for the texture being sharp may be the orientation relationship due to epitaxy (sample Nos. 31, 36), which is caused by the similarity in plane packing, FCC and HCP lattices, namely {100} and {10$\bar{1}$1}, {211} and {10$\bar{1}$0}, respectively. In the cases of synergistic action of the effects of textured substrate and electrochemical conditions rather sharp fibre textures were produced.

3.3. *Texture of zinc coatings electrodeposited on amorphous Ni–P alloy substrates*

Table 5 summarizes the electrodeposition conditions for zinc coatings on the amorphous substrate along with the specifications of the obtained texture components. It is natural to expect in the case of Ni–P amorphous substrates that the zinc coating texture will depend solely on the electrochemical conditions. Our investigations indicated the presence of simple fibre textures only and the absence of cone fibre texture. This result confirms once again that the reason for the appearance of cone textures is the epitaxial effect of textured substrates on which the Zn coatings have been electrodeposited, as described in the previous sections. Furthermore, it can be seen that the preferential orientation ⟨11$\bar{2}$0⟩ is obtained from bath ‘B’, with different sharpness levels according to the employed current density (Fig. 4, specimen No. 15). At higher current densities, D_c = 4 A dm^{-2}, the binary ⟨11$\bar{2}$0⟩ + ⟨10$\bar{1}$0⟩ orientation was obtained. Further increase in the cathode current density up to 8 A dm^{-2} resulted in an unoriented (random distribution) specimen.

Specimens with one sharpened ⟨10$\bar{1}$0⟩ orientation

Table 3. Texture ⟨uv.w⟩ of zinc coating of various thickness electrodeposited under different current conditions on cold worked copper substrates

Specimen No.	*Bath*	*Cathodic current density D_c (A dm^{-2})*	*Thickness of the deposit (μm)*	*Predominant orientation ⟨uv.w⟩*	*Type of texture and angle ϕ_0*	*Kind of electric current*
10	C	2	10	⟨10$\bar{1}$0⟩ + ⟨11$\bar{2}$0⟩	Cone text. 16°	Continuous
11	C	2	20	⟨10$\bar{1}$0⟩ + ⟨11$\bar{2}$0⟩	Cone text. 16°	Continuous
12	C	2	40	⟨10$\bar{1}$0⟩ + ⟨11$\bar{2}$0⟩	Cone text. 16°	Continuous (Fig. 3a and 3b)
13	C	2	20	⟨10$\bar{1}$0⟩ + ⟨11$\bar{2}$0⟩	Cone text. 16°	With pauses

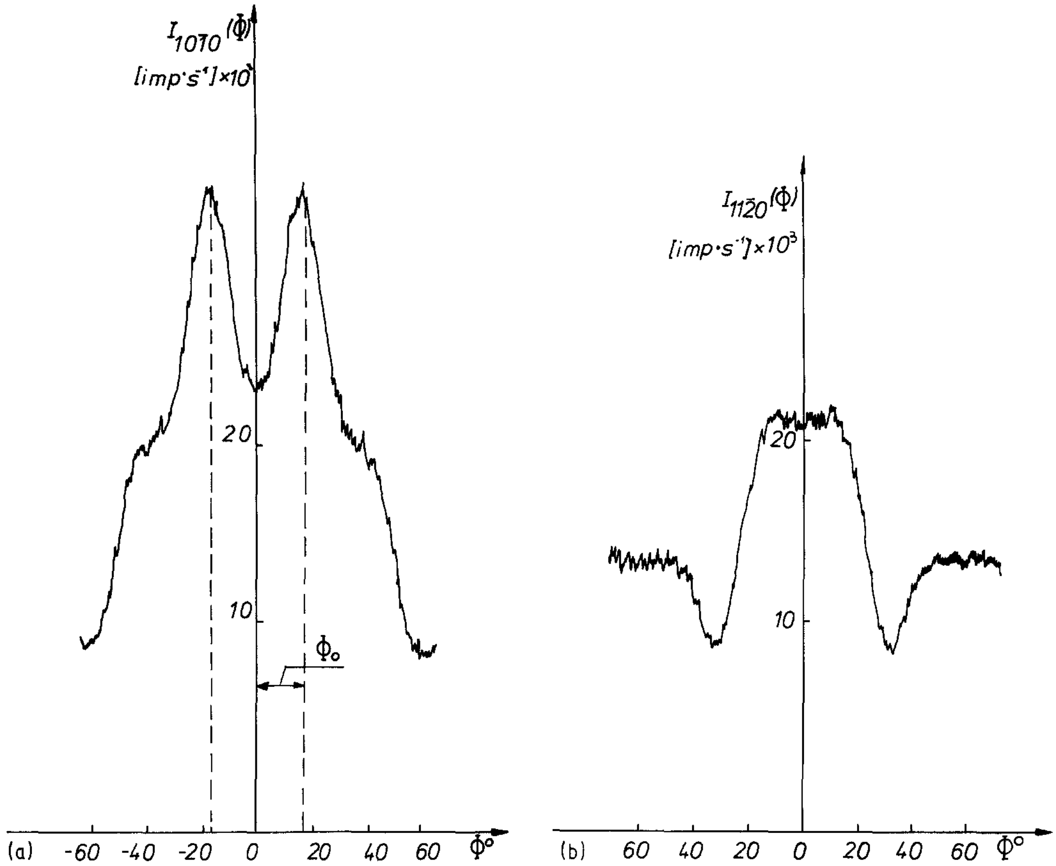

Fig. 3. Pole figures of zinc coating electrodeposited on cold worked copper substrate (sample 12, Table 3): (a) $\{10\bar{1}0\}$ and (b) $\{11\bar{2}0\}$. Bicomponential cone texture: $\langle 10\bar{1}0\rangle$ with $\phi_0 = 16°$ and $\langle 11\bar{2}0\rangle$, respectively. The symmetrical maxima of $\langle 11\bar{2}0\rangle$ component are overlapping on the $\{11\bar{2}0\}$ pole figure.

were obtained from the 'C' bath (brightener additive 'Univer B'), irrespective of the current density employed.

3.4. *Recrystallization of zinc coatings at room temperature*

We established that primary recrystallization occurred in some of the zinc coatings. This phase transition is completed relatively shortly after the electrolytic deposition ends. A similar phenomenon has been observed for electrodeposited copper coatings [8]. This effect held for specimens deposited both from chloride and sulphate baths. It was mainly found in specimens obtained from baths with no additives. It is known that the driving force of phase transformation is the storage energy due to imperfections (dislo-

Table 4. Texture $\langle uv.w\rangle$ of zinc coatings electrodeposited on electrolytic nickel substrates with different orientations. Thickness of the deposit ~ 20 μm

Specimen No.	*Bath*	*Cathodic current density D_c ($A\ dm^{-2}$)*	*Texture of the nickel substrate $\langle uvw\rangle$*	*Zinc coating*		
				Predominant orientation $\langle uv.w\rangle$	*Type of texture*	*Characteristic of texture*
22	C	4	⟨211⟩	$\langle 10\bar{1}0\rangle$	Fibre text.	Sharp
23	C	4	⟨110⟩	$\langle 10\bar{1}0\rangle$		
24	C	4	⟨100⟩	$\langle 10\bar{1}0\rangle$		
25	C	4	⟨210⟩	$\langle 10\bar{1}0\rangle$		
26	C	2	⟨211⟩	$\langle 10\bar{1}0\rangle$	Fibre text.	Sharp
27	C	2	⟨110⟩	$\langle 10\bar{1}0\rangle$		
29	C	2	⟨100⟩	$\langle 10\bar{1}0\rangle$		
30	C	2	⟨210⟩	$\langle 10\bar{1}0\rangle$		
31	C	1	⟨211⟩	$\langle 10\bar{1}0\rangle$	Fibre text.	Sharp
32	C	1	⟨110⟩	$\langle 10\bar{1}0\rangle$	Cone text.	$\phi_0 = 15°$
33	C	1	⟨100⟩	$\langle 10\bar{1}0\rangle$	Cone text.	$\phi_0 = 15°$
34	C	1	⟨210⟩	$\langle 10\bar{1}0\rangle$	Cone text.	$\phi_0 = 20°$
35	B	1	⟨211⟩	$\langle 11\bar{2}0\rangle$	Fibre text.	Sharp
36	B	1	⟨110⟩	$\langle 11\bar{2}0\rangle$	Fibre text.	Sharp
37	B	1	⟨100⟩	$\langle 10\bar{1}1\rangle$	Fibre text.	Sharp (Fig. 4)
38	B	1	⟨210⟩	$\langle 11\bar{2}0\rangle$	Fibre text.	Smeared out

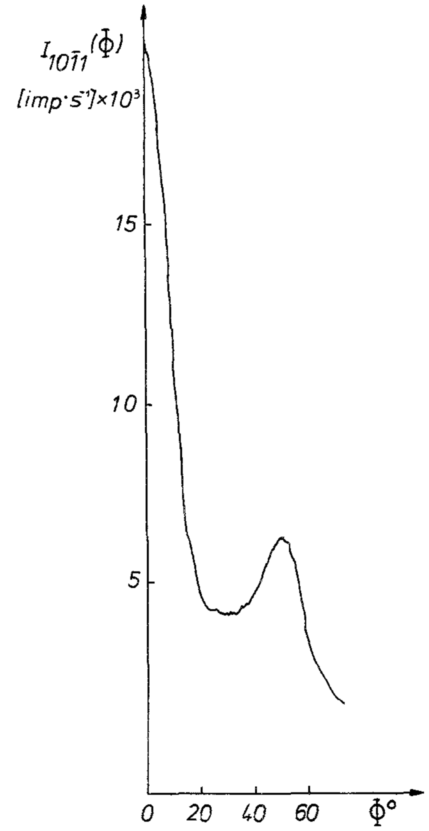

Fig. 4. Pole figure $\{10\bar{1}1\}$ of zinc coating electrodeposited on oriented ⟨100⟩ electrolytic nickel substrate (sample 37, Table 4). Texture component $\langle 10\bar{1}1 \rangle$.

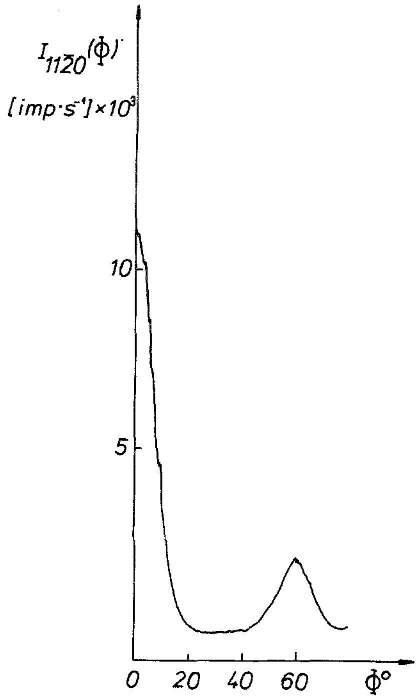

Fig. 5. Pole figure $\{11\bar{2}0\}$ of zinc coating electrodeposited on amorphous Ni–P substrate (sample 15, Table 5) – fibre texture with rather sharp component $\langle 11\bar{2}0 \rangle$.

cations and grain boundaries) of polycrystalline materials [12]. Figure 6 shows an example of recrystallization of a specimen prepared in a sulphate electrolyte. The continuous rings are from diffraction lines ⟨420⟩ and ⟨331⟩ of cold worked copper substrate. Other spot rings are due to recrystallized zinc, with Miller indices of $\langle 21\bar{3}2 \rangle$ and ⟨2131⟩.

4. Conclusions

(1) The experimental results show that the electrolysis parameters, bath composition and substrate texture affect the formation of zinc coating texture and, consequently, the physical and mechanical properties of the coatings associated with their anisotropy.

(2) Unoriented zinc deposits were obtained from the chloride electrolytes with no added inhibitors. Thus the hypothesis, as proposed for sulphate electrolytes [1], was confirmed, stating that the development of zinc coating textures is affected by an autoinhibitor, in this case the colloidal zinc hydroxide produced within the cathodic layer.

(3) The addition of synthetic inhibitors to the chloride electrolyte results in the development of various texture types, according to the cathodic current density and substrate structure. On cold worked copper substrates the zinc coatings were deposited with cone texture – presumably due to the packing inconsistency of the crystallographic planes. At higher densities of the deposition current, the ϕ_0 angle values were smaller, down to $D_c = 8\,A\,dm^{-2}$, when a simple fibre texture was obtained. When electrolytic nickel substrates with prescribed preferential orientations were used, various texture types were obtained in the deposited zinc coatings, depending on whether the electrochemical factors or epitaxial growth was the dominant influence. On the other hand, when zinc coatings were deposited on an

Table 5. Texture ⟨uv.w⟩ of zinc coating electrodeposited on amorphous Ni–P substrates. Thickness of the deposit ~20 μm

Specimen No.	Bath	Cathodic current density D_c $(A\,dm^{-2})$	Predominant orientation of the deposit ⟨uv.w⟩	Type of texture	Characteristic of texture
14	B	1	$\langle 11\bar{2}0 \rangle$	Fibre text.	Smeared out
15	B	2	$\langle 11\bar{2}0 \rangle$	Fibre text.	Rather sharp (Fig. 5)
16	B	4	$\langle 11\bar{2}0 \rangle + \langle 10\bar{1}0 \rangle$	Fibre text.	Sharp
17	B	8	Random	–	–
18	C	1	$\langle 10\bar{1}0 \rangle$	Fibre text.	Sharp
19	C	2	$\langle 10\bar{1}0 \rangle$	Fibre text.	Sharp
20	C	4	$\langle 10\bar{1}0 \rangle$	Fibre text.	Sharp

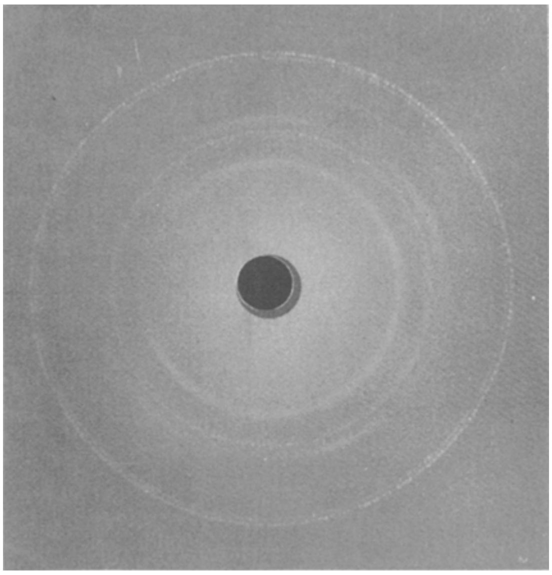

Fig. 6. X-ray back-reflection of recrystallizated zinc coating electrodeposited previously on cold worked copper substrate (CuK_α irradiation). Diffraction rings ⟨420⟩ and ⟨331⟩ of copper as well as $\langle 21\bar{3}2\rangle$ and $\langle 21\bar{3}1\rangle$ spot diffraction rings of recrystallized zinc are seen.

amorphous Ni–P alloy substrate, simple fibre textures were obtained irrespective of the electrolysis operating conditions.

(4) In zinc coatings electrodeposited from either chloride or sulphate baths, recrystallization processes at room temperature occur within a relatively short time. These processes are particularly evident in coatings deposited without synthetic inhibitors.

Acknowledgements

The authors are indebted to Mrs T. Bozinova for performing X-ray measurements. This work has been supported by the Polish Research Program CPBP 02.07 and the Institute of Physical Chemistry of the Bulgarian Academy of Sciences.

References

[1] V. Velinov, E. Beltowska-Lehman and A. Riesenkampf, *Surf. Coat. Technol.* **29** (1986) 77.
[2] G. Wasserman and J. Grewen, 'Texturen metallischer Werkstoffe', Springer, Berlin (1962) 18.
[3] S. Vitkova, J. Gancheva and G. Raichevsky, Proc. 6th Symposium on Electroplating, Budapest (1985) p. 381.
[4] N. Atanasov, Thesis, Institute of Physical Chem., Bulg. Acad. Sci., Sofia (1981).
[5] S. Rashkov and N. Atanasov, *Electrodep. Surf. Treat.* **3** (1975) 105.
[6] N. Atanasov, S. Vitkova and S. Rashkov, *Surf. Technol.* **13** (1981) 215.
[7] J. Amblard, Analyse des textures et mécanisme de l'électrocristalisation due nickel. Dr. Sci. Thesis, Univ. Pierre et Marie Curie, Paris VI (1976).
[8] I. V. Tomov, D. S. Stoychev and I. V. Vitanova, *J. Appl. Electrochem.* **15** (1985) 887.
[9] A. Riesenkampf, *Pr. Inst. Hutn.* **14** (1962) 27.
[10] A. Riesenkampf, *Freiberg. Forschungsh. B* **83** (1963) 80.
[11] A. Riesenkampf, *Electrochimiya* **7** (1971) 1633.
[12] A. L. Titchener and M. B. Bever, in 'Progress in Metal Physics', Vol. 7 (edited by B. Chalmers and R. King), Pergamon Press, London (1958).
[13] X. Shukai, H. Taishan and Z. Shaomin, *Chim. J. Chinese Univ. (English Edition)* **1** (1985) 9.